Polyhedron 117 (2016) 381–387

Contents lists available at ScienceDirect

Polyhedron

journal homepage: www.elsevier.com/locate/poly

Photoinduced oxidation reactions of the pendent macrocyclic complexes: Al(III) phthalocyanine and Ni(II) annulene mechanistic considerations

Guillermo Ferraudi [a,b,*], Alexander G. Lappin [b,*], Gustavo T. Ruiz [c], Betty Matsuhiro [d]

[a] Radiation Research Building, Univ. of Notre Dame, Notre Dame, IN 46556, United States
[b] Department of Chemistry and Biochemistry, Univ. of Notre Dame, Notre Dame, IN 46556, United States
[c] Instituto de Investigaciones Fisicoquímicas Teóricas y Aplicadas (INIFTA, UNLP, CCT La Plata-CONICET), Diag. 113 y 64, Sucursal 4, C.C. 16, (B1906ZAA) La Plata, Argentina
[d] Departamento de Ciencias del Ambiente, Facultad de Química y Biología, Universidad de Santiago de Chile, Av. B. O'Higgins 3363, Santiago, Chile

ARTICLE INFO

Article history:
Received 28 January 2016
Accepted 9 June 2016
Available online 16 June 2016

Keywords:
Pendent Ni(II) annulene complex
Pendent Al(III) phthalocyanine
Photoinduced redox processes
Saccharides oxidation
Kinetics and mechanism

ABSTRACT

The goal of the work was to expand the understanding of the photoinduced redox reactions of the Al(III) sulfonated phthalocyanine, HOAl^{III}tspc, and Ni(II) tertramethyldibenzotetraazaannnulene, [Ni^{II}(tmdbTAA)], as components of polymeric structures in which poly(ethyleneimino) and poly(isobutyl-alt-maleate) are the respective backbones of poly(HOAl^{III}tspc) and poly([Ni^{II}(tmdbTAA)]). Saccharide and flavonoid glycosides form adducts that quench the photo-generated oxidizing radicals in the case of poly(HOAl^{III}tspc) with rate constants $\approx 1 \times 10^4$ s^{-1}, largely independent of reductant structure. The charge-separated intermediate, CS, in the case of poly([Ni^{II}(tmdbTAA)]) shows greater reactivity with the saccharides and flavonoid glycosides, particularly with the flavonoid glycoside rutin where the rate constant is 2.7×10^6 s^{-1}. While phthalocyanine-centered radicals in poly(HOAl^{III}tspc) were reduced by dAMP (adenosine-5-monophosphate) and CT-DNA, energy transfer with these reagents competed with the formation of the CS intermediate in poly([Ni^{II}(tmdbTAA)]). A study of the intensity of the upper conversion luminescence ($\lambda_{em} < 500$ nm), modulated by the concentration of dAMP suggests that this is attributed to the formation of adducts of poly([Ni^{II}(tmdbTAA)]) with dAMP that affect the deactivation of the electronically excited Ni(II) tetraazaannnulene pendants before the formation of the CS intermediate.

1. Introduction

The extension of the redox photochemistry of metal macrocyclic complexes into the polymeric realm affords a number of interesting possibilities for cooperative interactions and unique chemistry [1–5]. Over the past several years, our laboratories have developed an interest in the two inorganic complex-containing polymers shown in Scheme 1. In poly(HOAl^{III}tspc), the pendant, pendant$^{\bullet 3-}$, Scheme 1 is charged and consequently there is an electrostatic barrier to cooperative interactions. Different interactions operate in the Ni-containing polymer where the [Ni^{II}(tmdbTAA-CO$\cdots$)] pendant is neutral and charge is distributed through the poly(isobutylenemaleate) backbone.

Although the pendants in both polymers are photoredox active, their photoprocesses are contrastingly different. It has been shown, that strands of poly(HOAl^{III}tspc) in aqueous solutions are associated in near spherical bundles with ~150 nm diameter, Fig. 1a. Most of the pendants in the bundles form π-stacks where the largest fraction of them are dimers. Redox active centers are photogenerated with visible light irradiation of the polymer [2,3]. Flash photochemical observations in a 0.15 ps to 100 μs time domain revealed the photogeneration of oxidized and reduced pendent radicals: pendant$^{\bullet 2-}$ and pendant$^{\bullet 4-}$. Both monomer and dimer forms of the phthalocyanine pendants are excited to their short lived singlet and triplet excited states, Eq. (1) and (2), which are then converted to

$$\text{pendant}^{3-} \xrightarrow{h\nu} \text{S or T}_{\text{pendant}^{3-}} \quad (1)$$

$$\{\text{pendant}^{3-}\,\text{pendant}^{3-}\} \xrightarrow{h\nu} \{\text{S or T}_{\text{pendant}^{3-}\,\text{pendant}^{3-}}\} \quad (2)$$

$$2\{\text{T}_{\text{pendant}^{3-}\,\text{pendant}^{3-}}\} \rightarrow \text{pendant}^{\bullet 4-} + \text{pendant}^{\bullet 2-} + 2\text{pendant}^{3-} \quad (3)$$

* Corresponding authors.
E-mail addresses: Ferraudi.1@nd.edu (G. Ferraudi), Lappin.1@nd.edu (A.G. Lappin), gruiz@inifta.unlp.edu.ar (G.T. Ruiz), bmatsuhiro@usach.cl (B. Matsuhiro).

http://dx.doi.org/10.1016/j.poly.2016.06.014
0277-5387/

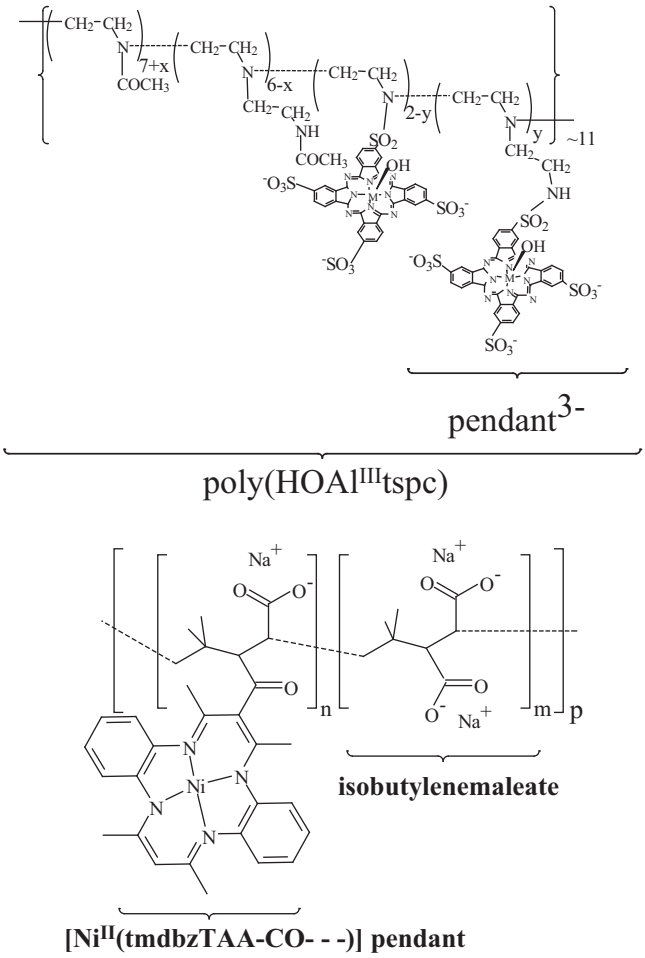

Scheme 1.

Phthalocyanine-centered radicals in processes occurring in microseconds, Eq. (3). The kinetics of the formation and disappearance of the radicals is consistent with energy and charge transfers between phthalocyanine pendants in the bundle. Radical scavengers such as methylviologen, O_2, catechol, and lignin, present in the solutions of poly(HOAl^{III}tspc) trapped the phthalocyanine radicals and demonstrate that scavenging reactions can compete with the slow radical-radical annihilation process and consequently, the polymers can be used to photocatalyze or photoinitiate redox processes. A comprehensive study of the poly([Ni^{II}(tmdbTAA)]) chemistry showed that the Ni(II) tetraazaannnulene complex grafted into poly(isobutylenemaleate) becomes soluble in aqueous and organic solvents where aggregates of strands have concentration and medium-dependent shapes, Fig. 1b. Irradiations of the polymer at $\lambda_{ex} = 532$ or 351 nm produce excited states, Eq. (4), which subsequently form charge-separated macrocyclic pendants, CS, with a lifetime, $\tau \sim 30$ ns, Eq. (5) [1].

$$\left[Ni^{II}(tmdbzTAA-\dot{\dot{C}}=O)\right] \xrightarrow[(\lambda_{ex}=532nm)]{+h\nu} \left[Ni^{II}(tmdbzTAA-\dot{\dot{C}}=O)\right]^{*} \quad (4)$$

$$\left[Ni^{II}(tmdbzTAA-\dot{\dot{C}}=O)\right]^{*} \rightarrow CS \quad (5)$$

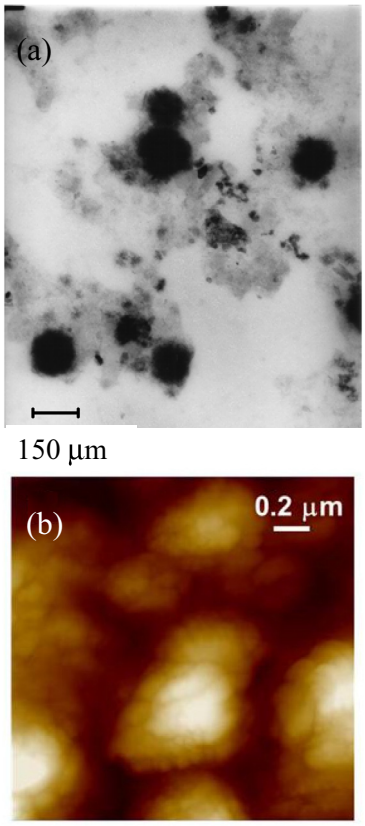

Fig. 1. Typical morphologies of strand aggregates of poly(HOAl^{III}tspc) and poly(Ni^{II}[tmdbzTAA])$_1$. A TEM picture of the polymer poly(HOAl^{III}tspc) spherical aggregates is shown in (a) . In (b), the structure of poly(Ni^{II}[tmdbzTAA])$_1$ observed with the AFM when the polymer is investigated in concentrated basic solutions. Z scale: (a) 300 nm. Scales are indicated in the figure. Complete morphological studies have been communicated in previous works [1–3].

In the absence of scavengers, the CS intermediate, formed with $\tau \sim 30$ ns, Eq. (5), decays with a lifetime $\tau \sim 1$ μs

$$2[Ni^{II}(tmdbzTAA-\dot{\dot{C}}=O)]^{*} \rightarrow [Ni^{II}(tmdbzTAA-\dot{\dot{C}}=O)] + [Ni^{II}(tmdbzTAA-\dot{\dot{C}}=O)]^{**} \quad (6)$$

Moreover, in parallel with the CS formation, exited state - exited state annihilation processes produce excited states that with a higher energy than the lowest lying excited state, Eq. (6).

The formation of such high energy excited states results in anti-Kasha luminescence, centered at ~430 nm of a higher energy than the excitation at $\lambda_{exc} \sim 530$ nm. Scheme 2 is a flow-diagram providing a simple visualization of the various excited states and their complex processes.

Various electron transfer reactions have shown that CS behaves as having a Ni(I) metal center and an oxidized tmdbTAA$^{\cdot -}$ ligand-radical. Both the phthalocyanine-based pendant$^{\cdot 2-}$ and the annulene-based CS react equally well with electron and hydrogen donors reconstituting the macrocyclic ligands. Because the annulene based CS has the dual roles of both oxidant and reductant, poly([Ni^{II}(tmdbTAA)]) photocatalyzes the endothermic reduction of CO_2 to CO when S(IV) species are present. The role of the S(IV) species is to reduce CS acting as sacrificial reagents. In the overall photocatalyzed process, the Ni(II) pendants fulfill the double role of antenna and catalyst.

In the present work, the focus is on the redox reactions of the photoexcited poly(HOAl^{III}tspc) and poly([Ni^{II}(tmdbTAA)])

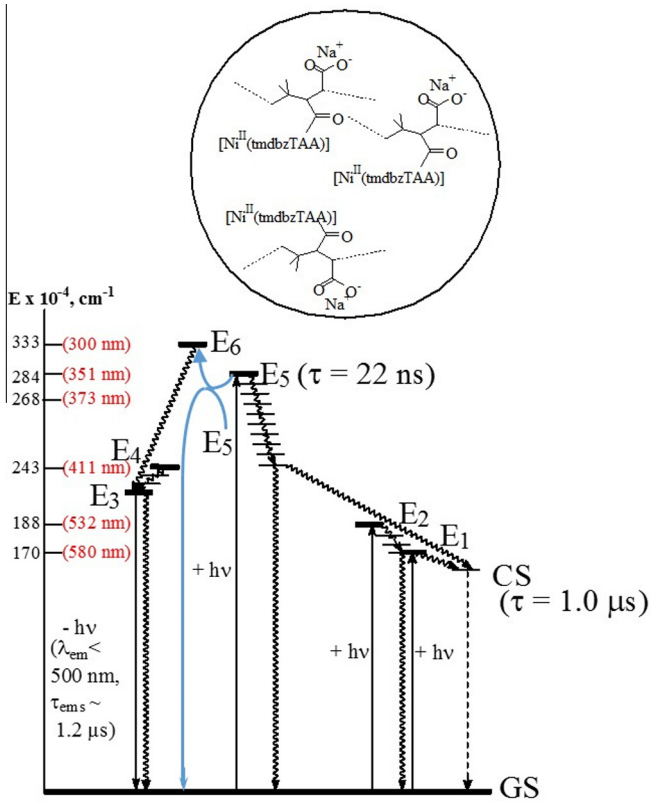

Scheme 2. A simpler nomenclature has been used to label the excited states (E_i, i = 1–6) whose properties were communicated in an earlier work [1]. The vertical axis shows relevant frequencies and wavelengths (in red). The E_5–E_5 annihilation producing the E_6 excited state is represented by the curved blue lines. Deactivation of E_5 and/or E_6 eliminates the channel leading to the formation of the charge separated intermediate, CS. The inset shows an idealized arrangement of [Ni^{II}(tmdbTAA-CO···)] pendants. Such sort of arrangement can be formed by intrastrand pendants and/or pendants from different strands in a bundle. Theoretical calculations have established that several structural factors contribute to the stability of the bundles [1]. (Color online.)

pendants with saccharide containing probes. The reactions of saccharides, flavonoid glycosides, Scheme 3, and more structurally complex probes dAMP (adenosine-5-monophosphate) and CT-DNA were used in the present mechanistic studies. The mechanisms of these relatively slow redox reactions were investigated in the ns to millisecond time domain using the time-resolved spectroscopic transformations associated with the formation and decay of pendant$^{\cdot 2-}$ and CS intermediates.

2. Experimental

2.1. Materials

Poly(HOAl^{III}tspc) and poly([Ni^{II}(tmdbTAA)]), mannitol, rutin, isoquercetin and quercetin were available from previous works and used as described [1–7]. The purity of the materials was verified by means of the UV–Vis absorption spectrum. Other materials were reagent grade and used as received. Sigma deoxy adenosine 5-monophosphate (dAMP) and calf thymus DNA (CT-DNA), fibrous preparation, highly polymerized were used as received.

2.2. Photochemical and photophysical procedures

Absorbance changes, ΔA, occurring on a time scale longer than 10 ns were investigated with a flash photolysis apparatus described elsewhere [8,9]. In these experiments, 10 ns flashes of 351 nm light were generated with a Lambda Physik SLL-200 excimer laser. The energy of the laser flash was attenuated to values equal to or less than 20 mJ/pulse by absorbing some of the laser light in a filter solution of $Ni(ClO_4)_2$ having the desired optical transmittance, $T = I_t/I_0$ where I_0 and I_t are respectively the intensities of the light arriving to and transmitted from the filter solution. The transmittance, $T = 10^{-A}$, was routinely calculated by using the spectrophotometrically measured absorbance, A, of the filter solution. A right angle configuration was used for the pump and the probe beams. Concentrations of poly(HOAl^{III}tspc) and poly([Ni^{II}(tmdbTAA)]) were adjusted to provide homogeneous concentrations of photogenerated intermediates over the optical path, l = 1 cm, of the probe beam. To satisfy this optical condition, solutions were made with an absorbance equal to or less than 0.8 over the 0.2 cm optical path of the pump.

Luminescence measurements were carried out in a fluorolog-3 apparatus. Deaerated solutions of poly([Ni^{II}(tmdbTAA)]) and poly (HOAl^{III}tspc) for either flash photolysis or luminescence measurements were prepared as communicated in previous work [3,8,9] and in the following section.

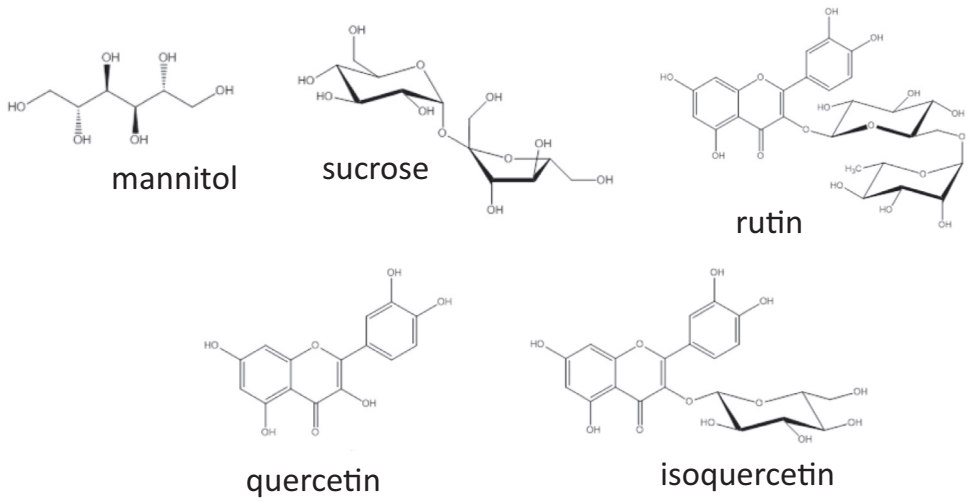

Scheme 3.

The concentrations of the various electron donors in these solutions are indicated elsewhere in the Section 3. All the solution used for the photochemical and photophysical experiments were deaerated with streams of ultrahigh purity N_2. A least squares method was used for fitting oscillographic traces to mono and biexponential functions. A fitting was considered unsatisfactory unless $\chi^2 \geqslant 0.995$.

2.3. Preparation of CT-DNA containing solutions

To prepare a stock solution of CT-DNA, a few threads of CT-DNA were dissolved in a freshly prepared pH 8 buffer solution. The resulting solution of CT-DNA was stirred for 5 h and left in a refrigerator overnight. The concentration of CT-DNA (in moles of base pairs per dm^3) was determined from the recorded spectrum of the solution at 260 nm ($\varepsilon = 6600\ M^{-1}\ cm^{-1}$). A concentration [CT-DNA] = 338 μM in base pair was calculated for the stock solution.

Equal volumes (~3 cm^3) of a stock solution of Poly(HOAl^{III}tspc) (1.8 mg in 200 cm^3 of the pH 8 buffer, absorbance at 351 nm, $A = 0.315$) and the stock CT-DNA solutions were mixed and kept in the refrigerator overnight. A 191.5 μM concentration (base pairs) of CT-DNA was calculated for the solution from a spectrophotometric analysis. Air was removed under vacuum from the solution used for the luminescence and flash photolysis experiments.

2.4. Preparation of the pH 8 buffer solution

BO_3H_3 (12.37 g) was dissolved in 100 cm^3 of 1 M NaOH. Aliquots of 1 M $HClO_4$ were added until a pH 8 was attained. Distilled water was subsequently added to reach the final volume of 1 dm^3.

3. Results

Spectroscopic evidence shows that the saccharide and flavonoid glycosides used in this work form adducts with both polymers, Supplementary Material and S1. The formation of such adducts causes significant mechanistic alterations of the transition metal complexes photoinduced redox reactions.

3.1. Photoinduced redox reactions of saccharide and flavonoid glycosides

Flash irradiation ($\lambda_{ex} = 532$ nm) of poly([Ni^{II}(tmdbTAA)]) in the presence of 0.1–0.05 M mannitol produces transient spectra previously associated with the formation of the Ni(I) pendants, [Ni^{I}(tmdbTAA-CO···)]$^-$, Fig. 2a [1].

The redox reaction of CS with mannitol bares a strong resemblance with the reduction of CS by trimethylamine, with a mechanism involving either an electron transfer or a proton-coupled electron transfer, Eq. (7) [1,10].

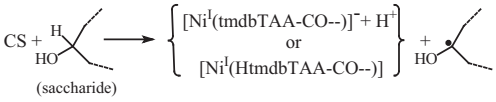

(7)

A similar redox process is observed when mannitol is replaced by 0.1–0.05 M concentrations of sucrose. The decay of the [Ni^{I}(tmdbTAA-CO···)]$^-$ pendants, whether they are produced by the reactions of CS with mannitol or sucrose, was observed on a longer time scale with a rate constant, k_r. Very similar values of k_r were calculated for the [Ni^{I}(tmdbTAA-CO···)]$^-$ decay in mannitol and sucrose containing solutions, Table 1.

Oscillographic traces showing the growth of the 360 nm absorbance of [Ni^{I}(tmdbTAA-CO···)]$^-$ were fit to a single exponential with a rate constant k_f, Table 1. It must also be noticed that the formation of [Ni^{I}(tmdbTAA-CO···)]$^-$ and its decay are both first order processes in [Ni^{I}(tmdbTAA-CO···)]$^-$ concentration and independent of scavenger concentration. The kinetics of these processes is consistent with a mechanism where the reaction occurs between adducts of the scavenger with the photoexcited pendant.

To investigate the reactions of the CS intermediate with the scavengers rutin, isoquercetin and quercetin, solutions of poly([Ni^{II}(tmdbTAA)]) containing 0.1–0.01 M of a given scavenger were flash irradiated at $\lambda_{ex} = 532$ nm. On a time scale $t < 60$ ns the transient spectrum recorded when either scavenger was present shows

Table 1
Rate constants of the scavenging, k_f, and the recovery, k_r, processes.

Scavengers	Poly(Altspc)		Poly(Ni^{II}[tmdbTAA])	
	k_f (s^{-1})	k_r (s^{-1})	k_f (s^{-1})	k_r (s^{-1})
Sucrose	1.1×10^4	6.1×10^3	8.5×10^4	4.8×10^2
Mannitol	7.5×10^3	4.8×10^3	7.0×10^4	1.5×10^3
Rutin	2.0×10^4	3.7×10^2	2.7×10^6	3.7×10^5
Isoquercetin	9.4×10^3	5.1×10^2	2.2×10^5	2.2×10^4
Quercetin [a]	$<1 \times 10^3$	–	$<1 \times 10^3$	–

[a] Reactions with CS and pendant^{-2} appear to be too slow for the maximum concentration of quercetin. Indeed, a slow reaction between quercetin and a more powerful oxidant, nitrosodisulfonate, communicated in the literature [12] lends support to this assertion.

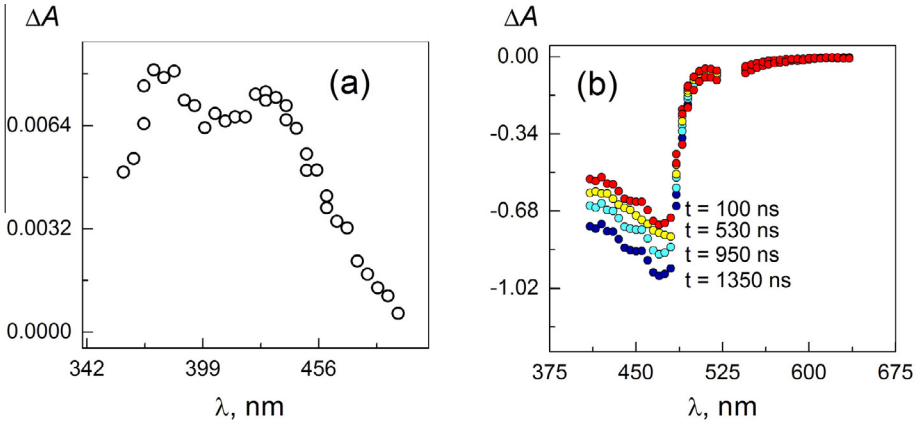

Fig. 2. Transient spectrum generated when a solution of poly([Ni^{II}(tmdbTAA)]) in the presence of 0.1 M mannitol is flash irradiated at $\lambda_{ex} = 532$ nm. The spectrum has been previously associated with the formation of the metal ion-reduced pendants, [Ni^{I}(tmdbTAA-CO$^-$···)]$^-$. (b) A bleach of the absorption band of the flavonoid glycoside group is observed at 470 nm when poly([Ni^{II}(tmdbTAA)]) and 0.1–0.01 M of a given scavenger were flash irradiated at $\lambda_{ex} = 532$ nm. In the figure, the scavenger used is rutin. A partial recovery of the absorbance is observed at longer times.

a bleach of the absorbance at 470 nm where the absorption band of the flavonoid glycoside group is placed, Fig. 2b. Because of the extinction coefficients of the flavonoid glycosides group are much larger than those of the $[Ni^{I}(tmdbTAA\text{-}CO\cdots)]^{-}$ pendants, there was not a good spectral window where changes in the concentration of Ni(I) pendants could be followed. The bleaching of the solution increases during the subsequent 100 ns to 1 μs period with an exponential dependence on time. Rate constants, $k_f = 2.7 \times 10^6$ and 2.2×10^5 s^{-1}, respectively, were calculated for the reactions with rutin and isoquercetin. Recovery of the bleached absorbance happens in the 1 μs to 1 ms period. Oscillographic traces of the absorbance recovery exhibit a single exponential dependence on time with rate constants $k_r = 3.7 \times 10^5$ and 2.2×10^4 s^{-1}, respectively, calculated for the reactions with rutin and isoquercetin. In contrast to rutin and isoquercetin scavengers, no reaction was observed with quercetin.

The pendant$^{\cdot 4-}$ and pendant$^{\cdot 2-}$ species were photogenerated in flash irradiations of poly($HOAl^{III}$tspc) solutions at 351 nm. They were detected by the transient UV–Vis spectra reported earlier [3]. In solutions where 0.1–0.01 M mannitol or 0.1–0.01 M sucrose were present, only the spectrum of the pendant$^{\cdot 4-}$ is observed due to the rapid scavenging of the pendant$^{\cdot 2-}$ by the saccharides, Fig. 3a. Oscillographic traces corresponding to the growth and decay of the pendant$^{\cdot 2-}$ spectrum were fitted to exponentials with rate constants that are almost one order of magnitude smaller than those obtained for the CS intermediate. In addition to the 351 nm photolysis of poly($HOAl^{III}$tspc), flash irradiations at $\lambda_{ex} = 532$ nm of solutions of the polymer containing 0.1–0.01 M concentrations of rutin, isoquercetin or quercetin were used for a study of the pendant$^{\cdot 2-}$ reactions with the flavonoid glycosides. When the quencher is rutin or isoquercetin, transient spectra recorded before the scavenging of pendant$^{\cdot 2-}$ by the flavonoid glycosides takes place, i.e., with delays equal to or shorter than 10^2 ns from the laser flash, the spectra show the presence of both the pendant$^{\cdot 4-}$ and pendant$^{\cdot 2-}$. On a longer time scale, i.e. 10^2 ns to 6 μs, the transient spectra changed into the combined spectrum of the pendant$^{\cdot 4-}$ and the corresponding flavonoid glycoside radical whose features were communicated in the literature, Fig. 3b [11,12]. When this process finishes, there is a subsequent partial recovery of the unphotolyzed solution spectra in a μs to ms time scale. It is the expected result if a stoichiometrically incomplete back reaction between the oxidized flavonoid glycoside and pendant$^{\cdot 4-}$ takes place. In contrast to the photoinduced reactions of rutin and isoquercetin, no reaction of the pendant$^{\cdot 2-}$ with quercetin was observed, Fig. 3b.

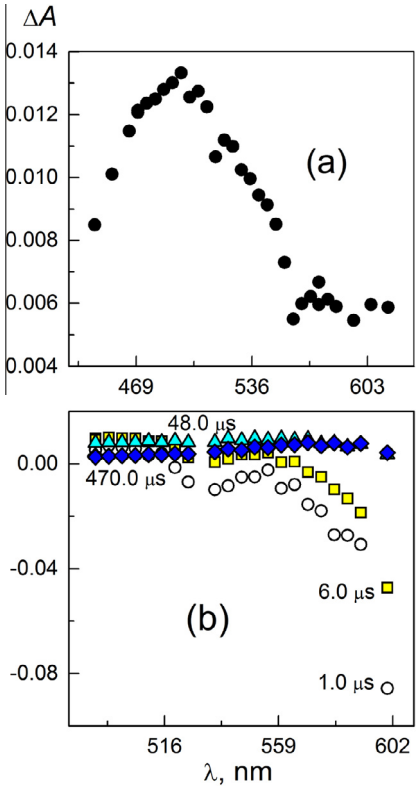

Fig. 3. (a) Only the spectrum of the pendant$^{\cdot 4-}$ instead of the combined spectrum of the pendant$^{\cdot 2-}$ and pendant$^{\cdot 4-}$ is observed when a solution of poly($HOAl^{III}$tspc) containing 0.1 M sucrose is flash irradiated at 532 nm. (b) In a 1–6 μs period, the transient spectrum changes into the combined spectrum of the pendant$^{\cdot 4-}$ and the flavonoid glycoside radical. A partial recovery of the (unphotolyzed) solutions spectra takes place in a longer than 6 μs time scale.

3.2. Processes (redox and photophysical) with dAMP and CT-DNA

To see whether the reactions of CS and pendant$^{\cdot 2-}$ with saccharides and flavonoid glycosides can also be observed with more complex molecules, the constituent sugars of deoxy adenosine 5-monophosphate, dAMP, and CT-DNA were used as reactants of the poly($[Ni^{II}$(tmdbTAA)]) and poly($HOAl^{III}$tspc) photoexcited pendants. To investigate these reactions, deaerated solutions containing CT-DNA or dAMP and a given polymer were flash irradiated at 351 nm. A comparison of the transient spectra observed when pendant$^{\cdot 4-}$ and pendant$^{\cdot 2-}$ are simultaneously photogenerated in a solution containing only poly($HOAl^{III}$tspc) and when the solution also contains 191.5 μM CT-DNA or 0.05 M dAMP shows that only the spectrum of the pendant$^{\cdot 4-}$ is observed in the presence of these scavengers. This spectroscopic difference is illustrated in Fig. 4 where the convolution of both pendant$^{\cdot 4-}$ and pendant$^{\cdot 2-}$ spectra is seen in the absence of dAMP and only the spectrum of the pendant$^{\cdot 4-}$ is recorded when it is present.

Compared with the spectrum of the pendant$^{\cdot 4-}$, the spectra of the radicals produced by the oxidation of dAMP have much smaller extinction coefficients leaving therefore the pendant$^{\cdot 4-}$ spectrum as the dominant observable optical change. A slow decay of the transient spectrum toward the base line is attributed to a back electron transfer reaction from the pendant$^{\cdot 4-}$ to radicals of the oxidized dAMP.

In contrast to the photobehavior of poly($HOAl^{III}$tspc) in solutions containing CT-DNA or dAMP, the spectra of $[Ni^{I}$(tmdbTAA-$CO\cdots)]^{-}$ and related transient species were not observed when poly($[Ni^{II}$(tmdbTAA)]) was flash irradiated at 351 nm in a solution containing 101 μM CT-DNA. In addition, the luminescence with $\lambda_{em} < 500$ nm from high energy excited states, a characteristic of the excited state of the pendents – excited state annihilation was absent [1]. The suppression of the poly($[Ni^{II}$(tmdbTAA)]) photoredox reactivity and photoluminescence is attributed to a quenching reaction. However the luminescence reappears in more dAMP concentrated solutions. A plot of the $I_e(0)/I_e$([dAMP]) where $I_e(0)$ and I_e([dAMP]) are respectively the emission intensity at 0 and the [dAMP] molar concentration is only linear at very low concentrations of dAMP, Fig. 5. Larger concentrations of dAMP result in higher luminescence intensities, namely I_e([dAMP]) > $I_e(0)$, causing a maximum in the graph. These experimental observations need to be interpreted in terms of two processes, one leading to an increase of the luminescence intensity and the other quenching it. The concentration and pH-induced morphological changes of poly($[Ni^{II}$(tmdbTAA)]) can be associated with rearrangements of the nickel chromophores with the corresponding effect on the intensity of the $\lambda_{em} < 500$ nm luminescence [1]. The morphological changes observed in the current study are attributed to the association of dAMP with poly($[Ni^{II}$(tmdbTAA)]). A good simulation of the curve $I_e(0)/I_e$([dAMP]) versus [dAMP] was obtained only when consideration was given to both, (a) equilibria between several

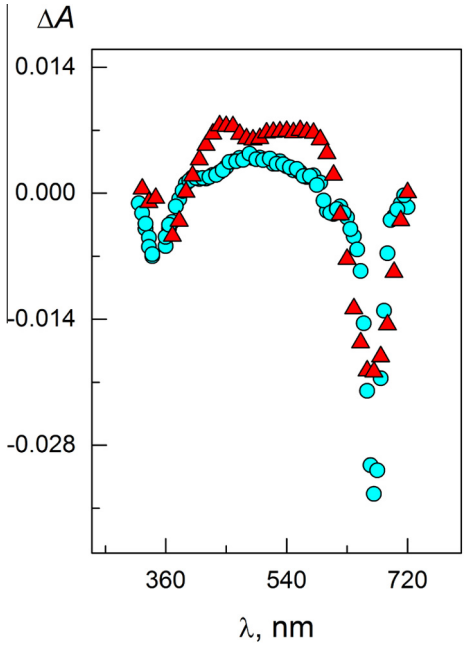

Fig. 4. Comparison of spectra (recorded both with equal delays from the photolysis flash) in the absence, Δ, and in the presence of CT-DNA, ○. The former spectrum is the convolution of the pendant$^{\cdot 2-}$ and pendant$^{\cdot 4-}$ spectra [3]. The latter spectrum shows the presence of the pendant$^{\cdot 4-}$ radical alone in the photolyzed solution. Differences between the two spectra demonstrate that a scavenging of pendant$^{\cdot 2-}$ by CT-DNA basis has taken place.

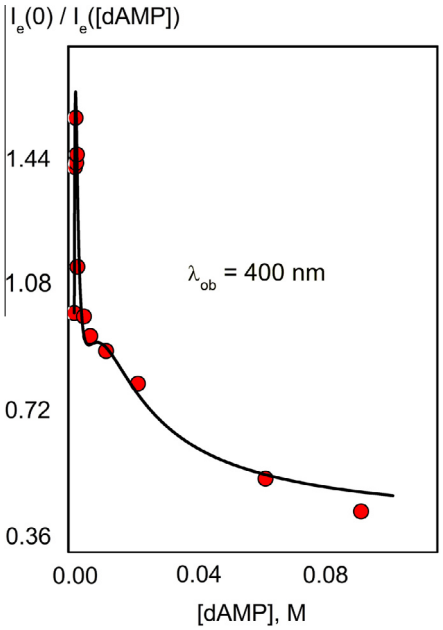

Fig. 5. The data points, ○, show the dependence of $I_e(0)/I_e([dAMP])$ on the dAMP concentration, [dAMP]. The emission of the poly([Ni^{II}(tmdbTAA)]) was followed at λ_{ob} = 465 nm when the deaerated solution was irradiated at 390 nm. A line plot simulates such a dependence. It was calculated on the assumption that the mechanism of the photoluminescene involves an equilibrium between four species consecutively formed when [dAMP] is varied between 0 and 0.1 M.

adducts with a different number of dAMP molecules attached to poly([Ni^{II}(tmdbTAA)]) and (b) different and intrinsic photophysical properties attributed to each of these adducts. A description of the mathematical simulation is in the Supplementary Material.

4. Discussion

The spectroscopic transformations observed after the photogeneration of either CS or pendant$^{\cdot 4-}$ and pendant$^{\cdot 2-}$ show that the scavengers; saccharides (mannitol and sucrose) and the glycosides (rutin and isoquercetin), are able to reduce CS and pendant$^{\cdot 2-}$. Both, the reduction of the pendants and the corresponding recovery exhibit first order kinetics. Since experimental observations show that they are independent of the scavenger concentration, the oxidation of the scavengers is kinetically of a first order in the CS and pendant$^{\cdot 2-}$ concentrations and of a zero order in the scavenger concentration. Also the recovery reactions exhibit the exponential dependence $e^{(-kr\ t)}$ of a rate of the recovery that is kinetically of a first order on the respective [Ni^{I}(tmdbTAA-CO$\cdots$)]$^{-}$ and pendant$^{\cdot 4-}$ concentrations. Indeed, the reduction products, [Ni^{I}(tmdbTAA-CO$\cdots$)]$^{-}$ or pendant$^{\cdot 4-}$, are produced in a 1:1 stoichiometric relation with the oxidized scavenger. A kinetic regime resembling that of a reaction that is kinetically of a second order is expected if a mobile, oxidized scavenger diffuses to the bulk of the solution before it reacts in the recovery process. Consequently, the experimentally observed first order kinetics of the scavenger oxidation and the recovery can be reconciled if one assumes that, prior to the oxidation, the pendants and the scavenger are affixed or the scavenger is trapped in pockets of the polymer. This is summarily shown in the Scheme 4.

Published observations made on the reactions of pulse radiolytically generated radicals with pendants in poly(HOAl^{III}tspc) showed that the reactants are affixed in pockets within the bundles of polymer strands [2]. This is consistent with the spectroscopy observations in the Supplementary Material. Since also traces showing the spectroscopic recovery in the reactions of the flavonoid glycosides are well fitted to mono exponentials, similar mechanistic considerations to those made for the saccharide scavengers can be made for the reduction of the pendants with flavonoid glycosides.

A comparison of the reaction rate constants based on the number of saccharide units in the scavengers shows that the rate constant of the reduction of the pendant$^{\cdot 2-}$ by rutin is almost two times larger than the rate constant of the reaction with the disaccharide sucrose. Similarly the rate constant of the reaction with isoquercetin is slightly larger, ~1.3 times, than the rate constant of the reaction with mannitol. Although the differences in the reaction rates of the pendant$^{\cdot 2-}$ with glycosides is small, a larger effect is seen in the reactions of CS where the rate constants of the reactions of CS with rutin and isoquercetin are respectively 32 and 3 times larger than the corresponding rate constant of the sucrose and mannitol reactions. Since reactions of the quercetin are slower than those of the glycosides, the acceleration in the reaction rates cannot be attributed only to the existence of parallel reactions of the flavonoid and saccharide groups of the flavonoid glycosides. It is possible that saccharide groups in the flavonoid glycosides assist in keeping the latter affixed to the poly([Ni^{II}(tmdbTAA)])

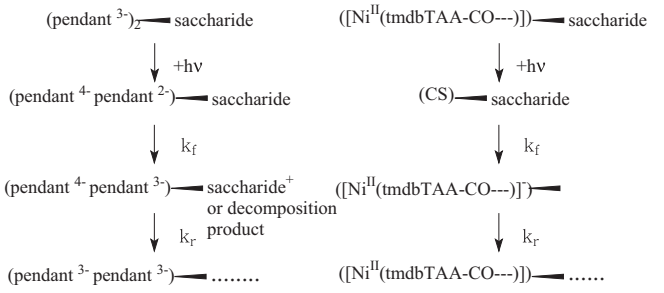

Scheme 4.

and poly([Ni^{II}(tmdbTAA$^{\cdot}$)])$^{+}$. In this case, the experimentally observed flavonoid glycoside radicals observed must be formed as secondary products. This process is described by Eqs. (15) and (16).

$$O^{\bullet} + F - G \xrightarrow{k_f} O + F - (G^{\bullet+}) \quad (O^{\bullet+} = \text{pendant}^{2-} \text{or CS}, F - G = \text{flavonoid glycoside}, \; F - (G^{\bullet+}) = \text{glycoside} - \text{centered radical}) \tag{15}$$

$$F - (G^{\bullet+}) \rightarrow (F^{\bullet+}) - G \quad ((F^{\bullet+}) - G = \text{flavonoid} - \text{centered radical}) \tag{16}$$

The Eq. (15) represents the oxidation of the glycoside group in the flavonoid glycoside species, while Eq. (16) is the formation of the flavonoid radical, glycoside-(flavonoid$^{\cdot+}$), observed in the flash photolysis experiments. Since the conversion of one radical to another, Eq. (16), is faster than Eq. (15), the Eq. (15) becomes the rate determining step of the flavonoid radical formation. A similar mechanism explains the photoreaction where poly(HOAl^{III}tspc) is the photolyte and dAMP is the scavenger of the pendant$^{\cdot2-}$ radical. In the dAMP case, the desoxyribose will be first oxidized and will transfer the oxidation to the adenine in a subsequent step.

Although the CS photogenerated from poly([Ni^{II}(tmdbTAA)]) is able to oxidize the saccharide and flavonoid glycoside compounds, it failed to oxidize CT-DNA. The failure to function as a photooxidant cannot be attributed to an inadequate redox potential because the excited state and CS spectra reported in the literature would have been observed in the flash photolysis experiments. A mechanism involving energy transfer accounts for the complex dependence of the poly([Ni^{II}(tmdbTAA)]) luminescence on dAMP concentration and the lack of photoredox activity. In order for the energy transfer processes to deactivate excited states, the energy transfers to dAMP must occur from excited states above the lowest excited state of the nickel(II) pendants, i.e., the channel leading to the formation of CS, Scheme 2. These excited states must be upper energy excited states participating or being formed in the excited-excited state annihilation process, Eq. (6). They are the electronic state precursors of the CS and responsible for the $\lambda_{em} < 500$ nm poly([Ni^{II}(tmdbTAA)]) luminescence [1]. Interestingly, under these energetic restrictions there is a strong resemblance between the dAMP quenching of the respective poly([Ni^{II}(tmdbTAA)]) and 9-aminoacridine luminescence [13]. Yet, this quenching mechanism alone cannot explain the tuning of the emission intensity by dAMP, Fig. 5. As the dAMP concentration increases, adducts incorporating a greater number of dAMP molecules attached poly([Ni^{II}(tmdbTAA)]) must be formed inducing morphological changes. Indeed, the effect of the medium and concentration-dependent morphology on some properties of poly([Ni^{II}(tmdbTAA)]) was previously established [1]. Some strand adducts will have arrangements of pendants with a more intense luminescence than other adducts of poly([Ni^{II}(tmdbTAA)]). The luminescence intensity therefore follows the intrinsic photophysical properties of each dAMP – poly([Ni^{II}(tmdbTAA)]) adduct. Morphologies benefiting the non-luminescent excited states E_1 and/or E_2 must not be produced since they will also lead to the formation of the CS intermediate. Displacements of equilibria between various morphologies must also be included to explain the dependence of $I_e(0)/I_e$([dAMP]) on [dAMP], Supplementary Material and S2.

In contrast to poly([Ni^{II}(tmdbTAA)]), the excited states of poly(HOAl^{III}tspc) decay in a shorter time scale forming the reactive pendant$^{\cdot4-}$ and pendant$^{\cdot2-}$ phthalocyanine radicals [2,3]. The fast decay of the excited states forming the pendant$^{\cdot4-}$ and pendant$^{\cdot2-}$ radicals will make for an inefficient transfer of energy to the bases of CT-DNA and dAMP and allow the redox processes of pendant$^{\cdot4-}$ and pendant$^{\cdot2-}$ to proceed forward. Additionally the time scale and kinetics of these processes is consistent with the formation of adducts between the saccharide containing reactants and polymers.

5. Conclusions

In spite of the structural and charge differences, the photoinduced oxidation reactivity of poly([Ni^{II}(tmdbTAA)]) and poly(HOAl^{III}tspc) show significant similarities. The pendents in both polymeric species form adducts with saccharide and flavonoid glycosides that are responsible for the electron-transfer behavior and the photo-products show no evidence for diffusion from the polymer. This is consistent with the saccharide units affixed to or trapped in pockets of the polymer. Differences are observed with the more complex reagents CT-DNA and dAMP. While poly(HOAl^{III}-tspc) shows reactivity similar to that of the simpler sugars, the more complex photochemistry of poly([Ni^{II}(tmdbTAA)]) results in a competitive energy-transfer quenching reaction of excited states. The work expands knowledge of the range of sacrificial reductants useful with these polymeric reagents and where poly([Ni^{II}(-tmdbTAA)]) has been employed in the photoinduced reduction of CO_2 to CO [1]. In prior work, inorganic S(IV) was used as the sacrificial reagent, but the findings of this work suggest that agricultural wastes rich in carbohydrates might also be used.

Acknowledgments

Part of this work was carried out in the Notre Dame Radiation Laboratory (NDRL). The NDRL is supported by the Division of Chemical Sciences, Geosciences and Biosciences, Basic Energy Sciences, Office of Science, United States Department of Energy through Grant number DE-FC02-04ER15533. This is contribution number NDRL 5055. G.T.R thanks to ANPCyT for funding (PICT 1435), UNLP and the Office of Research, University of Notre Dame for funding and hosting him there. G.T.R is a Research Member of CONICET, Argentina.

Appendix A. Supplementary data

Supplementary data associated with this article can be found, in the online version, at http://dx.doi.org/10.1016/j.poly.2016.06.014.

References

[1] G. Estiu, G. Ferraudi, A.G. Lappin, G.T. Ruiz, C. Vericat, J. Costamagna, M. Villagran, RSC Adv. 4 (2014) 53157 (and references therein).
[2] G.T. Ruiz, G. Ferraudi, A.G. Lappin, J. Photochem. Photobiol. A Chem. 206 (2009) 1.
[3] G.T. Ruiz, A.G. Lappin, G. Ferraudi, J. Polym. Sci. Part A 50 (2012) 2507.
[4] G.T. Ruiz, A.G. Lappin, G. Ferraudi, Porphyrins Phthalocyanines 14 (2010) 70.
[5] L.L.B. Bracco, M.P. Juliarena, G.T. Ruiz, M.R. Feliz, G.J. Ferraudi, E. Wolcan, J. Phys. Chem. B 112 (2008) 11506.
[6] S. Torres, G. Ferraudi, M.J. Aguirre, M. Isaacs, B. Matsuhiro, N.P. Chandía, L. Mendoza, Helv. Chim. Acta 94 (2011) 293.
[7] S. Torres, G. Ferraudi, N.P. Chandía, B. Matsuhiro, J. Coord. Chem. 64 (2011) 377.
[8] S. Thomas, G. Ruiz, G. Ferraudi, Macromolecules 39 (2006) 6615.
[9] J. Guerrero, O.E. Piro, E. Wolcan, M.R. Feliz, G. Ferraudi, S.A. Moya, Organometallics 20 (2001) 2842.
[10] M.H.V. Huynh, T.J. Meyer, Chem. Rev. 107 (2007) 5004.
[11] C. Cren-Olive, P. Happiot, J. Pinson, C. Rolando, J. Am. Chem. Soc. 124 (2002) 14027.
[12] S. Hodaka, R. Komatsu-Watanabe, T. Ideguchi, S. Sakamoto, K. Ichimori, K. Kanaori, K. Tajima, Chem. Lett. 36 (2007) 1388.
[13] Y. Kubota, Chem. Lett. (1977) 311.